Plasmon scattering approach to energy exchange and high frequency noise in nu=2 quantum Hall edge channels

Pascal Degiovanni, Charles Grenier, Gwendal Fève, Carles Altimiras, Hélène Le Sueur, Frédéric Pierre

▶ **To cite this version:**

HAL is a multi-disciplinary open access archive for the deposit and dissemination of scientific research documents, whether they are published or not. The documents may come from teaching and research institutions in France or abroad, or from public or private research centers.

L'archive ouverte pluridisciplinaire **HAL**, est destinée au dépôt et à la diffusion de documents scientifiques de niveau recherche, publiés ou non, émanant des établissements d'enseignement et de recherche français ou étrangers, des laboratoires publics ou privés.

Plasmon scattering approach to energy exchange and high frequency noise in $\nu = 2$ quantum Hall edge channels

P. Degiovanni[1], Ch. Grenier[1], G. Fève[2], C. Altimiras[3], H. le Sueur[3], and F. Pierre[3]

(1) Université de Lyon, Fédération de Physique André Marie Ampère,
CNRS - Laboratoire de Physique de l'Ecole Normale Supérieure de Lyon, 46 Allée d'Italie, 69364 Lyon Cedex 07, France
(2) Laboratoire Pierre Aigrain, Département de Physique de l'Ecole Normale Supérieure,
24 rue Lhomond, 75231 Paris Cedex 05, France and
(3) CNRS, Laboratoire de Photonique et de Nanostructures (LPN) - Phynano team, Route de Nozay, 91460 Marcoussis, France

Inter-edge channel interactions in the quantum Hall regime at filling factor $\nu = 2$ are analyzed within a plasmon scattering formalism. We derive analytical expressions for energy redistribution amongst edge channels and for high frequency noise, which are shown to fully characterize the low energy plasmon scattering. In the strong interaction limit, the predictions for energy redistribution are compared with recent experimental data and found to reproduce most of the observed features. Quantitative agreement can be achieved by assuming 25% of the injected energy is lost towards other degrees of freedom, possibly the additional gapless excitations predicted for smooth edge potentials.

Electronic transport along the chiral edges of a two dimensional electron gas (2DEG) in the Quantum Hall (QH) regime can now be studied using a single electron source [1], thus opening the way to fundamental electron optics experiments such as single electron Mach-Zenhder interferometry (MZI) [2] or Hong-Ou-Mandel experiments [3]. However, contrary to photons, electrons strongly interact through the Coulomb interaction. This leads to relaxation and decoherence phenomena and thereby questions the whole concept of electron quantum optics. The $\nu = 2$ filling factor is particularly appropriate to address this issue since the electromagnetic environment of one edge channel (EC) mainly consists of the other EC. In this respect, it is an ideal test bed to investigate interaction effects in the QH regime.

Coulomb interactions lead to plasmon scattering which in turn basically determines the linear transport properties of one dimensional systems: finite frequency admittances [4] and thermal conductivity [5, 6]. Recently it was pointed out as a key ingredient for understanding the interference contrast of Mach-Zehnder interferometers at $\nu = 2$ [7] and single electron relaxation along ECs [8]. However, despite its fundamental role in the QH regime low energy physics, plasmon scattering has only been indirectly probed through electron quantum interferences (MZI) [9, 10, 11, 12]. Recent progresses in the measurements of high frequency admittance [13, 14], noise [15] and electron distribution function [16] in these systems open new complementary ways to probe the dynamics of QH ECs.

In this letter, we discuss how energy relaxation and high frequency noise provide direct information on plasmon scattering in a $\nu = 2$ EC system. We anticipate it will permit us to reach a much deeper understanding of the low energy physics of the QH regime. The model considered here neglects possible additional excitation modes associated with the internal structure of ECs [18, 19, 20]. We derive from general considerations a universal expression for plasmon scattering that is valid at low energies. It gives the finite frequency admittances in the 6-terminal geometry depicted in Fig. 1 and energy exchanges between the two ECs. The latter are compared with experimental data recently obtained from electron relaxation in one of the edges of the $\nu = 2$ system [17] thus providing a quantitative test of plasmon scattering models. This comparison suggests that our model captures most of the physics of this system. We argue that the discrepancy between raw data and predictions might be due to energy leak in the predicted internal modes [19, 20]. Noise measurements in the GHz range provide more information on plasmon scattering and regarding the limits of our model as well as of another approach [24] based on iterating collision corrections to the free electron model [21].

Within the bosonization formalism, the $\nu = 2$ QH ECs are described using a two component bosonic field $\Phi = (\phi_\alpha)$ encoding plasmon modes of the outer ($\alpha = 1$) and inner ($\alpha = 2$) channels. It is related to the electronic densities by : $(\psi_\alpha^\dagger \psi_\alpha)(x) := (\partial_x \phi_\alpha)(x)/\sqrt{\pi}$. The effect of interactions between $x = 0$ and $x = L$ is conveniently described in terms of a scattering matrix $\mathbf{S}(\omega, L)$ relating incoming ($x = 0$) and outgoing ($x = L$) plasmon modes with frequency $\omega/2\pi$ [25]. Denoting by $\Phi(\omega, x)$ the Fourier transform of the two component field Φ with respect to time, $\mathbf{S}(\omega, L)$ is defined as

$$\Phi(\omega, L) = \mathbf{S}(\omega, L) . \Phi(\omega, 0) . \tag{1}$$

Let us now derive a universal form for $\mathbf{S}(\omega, L)$ valid at low energies.

We first consider the situation where the two QPCs shown in Fig. 1 are set to fully transmit the outer EC and fully reflect the inner one. Then, the plasmon scattering matrix element $\mathbf{S}_{\alpha,\beta}(\omega, L)$ is related to the sample admittance [14, 22] between contacts $i = \alpha'$ and $j = \beta$
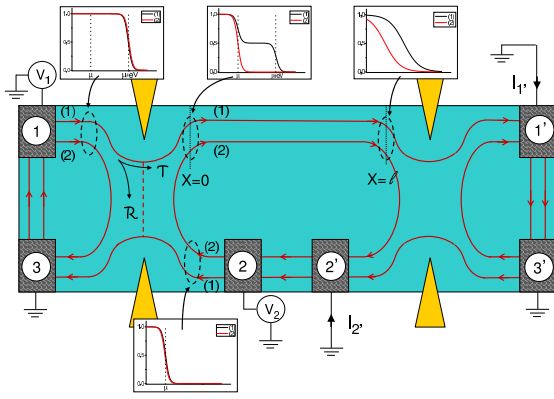
FIG. 1: (Color online) Relaxation of a non equilibrium distribution created in EC (1) by a QPC of transmission $\mathcal{T}$, biased at V (here $\mathcal{T} = 0.5$). Edge channels (1) and (2) interact between $x = 0$ and $x = L$. The electron distribution function in channel (1) evolves from a non equilibrium smeared double step to a thermal-like distribution function. The right QPC is set to perfectly reflect (transmit) the internal (external) EC. For admittance measurements, the left QPC is operated as the right one. Voltage drives $V_{1,2}(t)$ are applied and currents $I_{1',2'}(t)$ are measured at contacts $1'$ and $2'$.

as depicted on Fig. 1:

$$G_{i,j}(\omega, L, B_\perp) = -\frac{e^2}{h} \mathbf{S}_{\alpha,\beta}(\omega, L). \qquad (2)$$

Here $B_\perp$ is the applied perpendicular magnetic field. Now, using the Onsager-Büttiker relations [23] $G_{i,j}(\omega, L, B_\perp) = G_{j,i}(\omega, L, -B_\perp)$ and the mapping $(\alpha, \beta') \mapsto (\alpha', \beta)$ when $B_\perp \mapsto -B_\perp$ that follows from the reversed propagation direction, we obtain that the plasmon scattering matrix is symmetric. Energy conservation implies that $\mathbf{S}(\omega, L)$ is a unitary matrix. Consequently, $\mathbf{S}(\omega, L)$ is of the form:

$$\mathbf{S}(\omega, L) = e^{i\theta(\omega, L)} \times e^{-i(a_z(\omega, L)\sigma^z + a_x(\omega, L)\sigma^x)} \qquad (3)$$

where $\theta(\omega, L)$ and $a_{x,z}(\omega, L)$ are real numbers independent of $B_\perp$ and $\sigma^{x,z}$ denote the Pauli matrices. At fixed frequency, $\mathbf{S}(\omega, L)$ goes to the identity for $L \to 0$. For propagation distances much larger than the interaction range, interactions can be viewed as local and therefore, scattering obeys $\mathbf{S}(\omega, L_1 + L_2) = \mathbf{S}(\omega, L_1).\mathbf{S}(\omega, L_2)$. Since $\mathbf{S}(\omega, L)$ goes to the identity at $\omega \to 0$, it is sufficient to expand $\theta(\omega, L)$ and $a_{x,z}(\omega, L)$ at first order in ω and we finally get:

$$\mathbf{S}(\omega, L) = e^{i\omega L/v_0} \times e^{-i\frac{\omega L}{v}(\cos(\theta)\sigma^z + \sin(\theta)\sigma^x)} \qquad (4)$$

where v_0 and v are velocities which, together with the angle θ completely determine plasmon scattering. The velocities of the plasmon eigenmodes in an infinite system are $v_\pm^{-1} = v_0^{-1} \pm v^{-1}$. The case of uncoupled channels corresponds to $\theta \equiv 0 \pmod{\pi}$ whereas any other

value corresponds to an interacting problem. The opposite limit $\theta \equiv \pi/2 \pmod{\pi}$ corresponds, within a microscopic model approach [7], to either equal channel velocities or strong inter-channel interactions.

Besides finite frequency admittances, plasmon scattering also determines energy redistribution between the two channels as a function of propagation distance. A plasmon of energy $\hbar\omega$ along a distance L has probability $T(\omega, L) = |\mathbf{S}_{11}(\omega, L)|^2$ to be transmitted in the same EC and $R(\omega, L) = |\mathbf{S}_{12}(\omega, L)|^2$ to be scattered into the other channel. The transmission probability oscillates with frequency: $T(\omega, L) = T_\infty + R_\infty \cos(2\omega L/v)$ where $T_\infty = 1 - R_\infty = (1 + \cos^2(\theta))/2$. In the large L limit, the energy injected in one EC through a broadband spectrum of plasmon excitations will be redistributed according to the coarse grained scattering probabilities T_∞ and R_∞. Since in the strong coupling limit, $T_\infty = R_\infty = 1/2$, this approach predicts asymptotic equipartition of energy between the two ECs in the limit $L \to \infty$.

To study the energy relaxation, let us consider the energy current along each EC. It is expressed in terms of the electron distribution function $f_\alpha(\varepsilon, x)$ in channel α at position x as

$$J_\alpha(x) = \int v_\alpha \rho_\alpha (f_\alpha(\varepsilon, x) - \Theta(\varepsilon)) \varepsilon \, d\varepsilon \qquad (5)$$

where v_α and ρ_α respectively denote the electron velocity and the density of states per unit of length and energy in channel α (in 1D systems $v_\alpha \rho_\alpha = 1/h$) and ε denotes the energy difference with the corresponding Fermi energy μ_α.

Within the bosonization formalism, the energy current is expressed in terms of the plasmon modes occupation numbers $\bar{n}_\alpha(\omega, x)$ in channel α at energy $\hbar\omega$ and position x:

$$J_\alpha(x) = \int_0^{+\infty} \hbar\omega \, \bar{n}_\alpha(\omega, x) \frac{d\omega}{2\pi}. \qquad (6)$$

In the setting depicted on Fig. 1, the initial plasmon occupation numbers within both channels are obtained from the finite frequency edge current noise injected by the QPC in each EC:

$$\bar{n}_\alpha(\omega, 0) = \frac{2\pi}{e^2} \frac{(\delta S)_{i_\alpha(0)}(\omega)}{\omega} \qquad (7)$$

where $(\delta S)_{i_\alpha(0)}(\omega) = S_{i_\alpha(0)}(\omega) - \frac{e^2}{4\pi}\omega$ is the difference of the finite frequency symmetric current noise and the zero point fluctuations.

As shown in the top-middle inset of Fig. 1, the outer channel is populated by a double step electron distribution characterized by the bias voltage V, the QPC transmission $\mathcal{T}$ and the temperature T_{el}. Consequently, the energy current injected into the outer channel is the sum of a thermal contribution given by [6]:

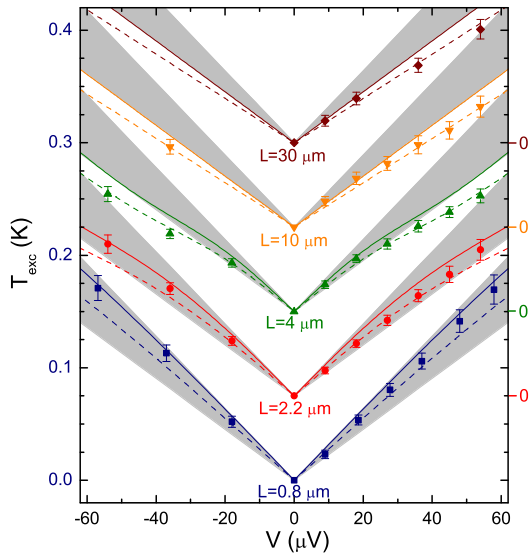$$J_{\alpha=1}^{(th)}(T_{el}) = \frac{\pi^2}{6h} (k_B T_{el})^2, \qquad (8)$$

FIG. 2: Comparison data-prediction for T_{exc} plotted vs the bias voltage V applied to a QPC set to $\mathcal{T} = 0.5$. A 75 mK vertical shift separates consecutive L. Symbols are data points [17]. Continuous lines are predictions of Eq. (10) with the known values of T, V, L, $\mathcal{T}$, assuming $T_\infty = 1/2$ and velocity $v = 10^5$ m/s. Dashed lines are the same predictions scaled down by 13%. Grey areas encapsulate values of $T_{\text{exc}}(V, \mathcal{T} = 0.5)$ accessible from Eq. (10).

and of an excess contribution associated through Eqs. (6) and (7) with the edge current excess noise:

$$S_{i_1(0)}^{(\text{exc})}(\omega) = e^2 \mathcal{R}\mathcal{T} \int_{-\infty}^{+\infty} (\delta f)_{V,T_{\text{el}}}(\omega')(\delta f)_{V,T_{\text{el}}}(\omega+\omega')\frac{d\omega'}{2\pi},$$
(9)

where $\mathcal{R} = 1 - \mathcal{T}$ and $(\delta f)_{V,T_{\text{el}}}(\omega) = f_{T_{\text{el}}}(\hbar\omega + eV) - f_{T_{\text{el}}}(\hbar\omega)$ denotes a difference of Fermi functions at temperature T_{el}.

Since a thermal distribution at temperature T_{el} is injected into the inner channel, the thermal part of the energy current in the outer channel is left unchanged by propagation along a distance L. On the contrary, the excess noise is attenuated by $T(\omega, L)$. This finally leads to the excess contribution to the energy current in the outer channel at $x = L$ which we now express as an excess temperature T_{exc} as in Eq. (8):

$$\left(\frac{k_B T_{\text{exc}}}{eV}\right)^2 = \frac{3\mathcal{T}\mathcal{R}}{\pi^2}\left(T_\infty + R_\infty \frac{\text{sinc}^2(L/L_V)}{\text{sinhc}^2(2\pi L/L_{\text{th}}(T_{\text{el}}))}\right)$$
(10)

where $\text{sinc}(x) = \sin(x)/x$, $\text{sinhc}(x) = \sinh(x)/x$. The length scales $L_V = \hbar v/e|V|$ and $L_{\text{th}}(T_{\text{el}}) = v\hbar/k_B T_{\text{el}}$ respectively associated with the bias voltage and temperature govern the L dependence. This expression interpolates between the initial $L = 0$ value $(3/\pi^2)\mathcal{R}\mathcal{T}$ and the asymptotic value $(3/\pi^2)\mathcal{R}\mathcal{T}T_\infty$.

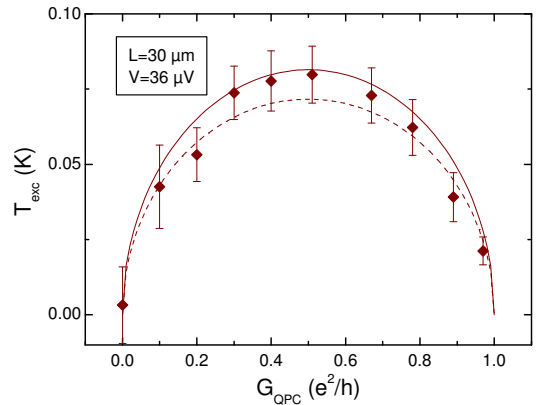We now confront our quantitative predictions with experimental data. In the very recent experiment [17] per-

FIG. 3: Comparison data-prediction for $T_{\text{exc}}(\mathcal{T})$. Symbols are data points vs $G_{QPC} = \mathcal{T}e^2/h$ obtained at $L = 30$ μm and $V = 36$ μV in a different run than [17], after a thermal cycle to room temperature. The continuous line is the $L = \infty$ prediction of Eq. 10 with $T_\infty = 1/2$. The dashed line is the same prediction scaled down by 13%.

formed on a typical GaAs/Ga(Al)As semiconductor heterojunction set to Landau level filling factor 2, T_{exc} is extracted from measurements of the electronic energy distribution function. First, Fig. 2 shows as symbols T_{exc} plotted vs the QPC bias V for a fixed transmission $\mathcal{T} = 0.5$. In the strong interaction limit $T_\infty = 1/2$, and using the velocity $v = 10^5$ m/s, eq. (10) reproduces the characteristic energy relaxation length as well as the observed non-linear shape of $T_{\text{exc}}(V)$, most pronounced for $L = 4$ μm. A quantitative discrepancy remains at $L \geq 4$ μm, which can not be accounted for within our theoretical framework as data points are outside the grey areas. This suggests that additional degrees of freedom are involved, such as internal modes of ECs [20]. Energy transfers to these modes was not ruled out by experiment for the inner EC, expected wider and therefore more prone to such phenomena than the outer EC. We find a good quantitative agreement with the data at $L \geq 4$ μm by applying a 13% reduction to the predicted T_{exc}, which corresponds to the absorption of 25% of the injected energy by additional degrees of freedom (dashed lines). Second, figure 3 shows as symbols T_{exc} vs $\mathcal{T}$ obtained after a large energy relaxation, at $L = 30$ μm. We find that the predicted proportionality of $T_{\text{exc}}(\mathcal{T})$ with $\sqrt{\mathcal{T}(1-\mathcal{T})}$ is obeyed. Note that in this experimental run different from [17], the larger uncertainty would hide the 13% discrepancy observed above.

To get a better understanding of this discrepancy, it would be very useful to measure the frequency dependance of the plasmon transmission probability $T(\omega, L)$ as well as the probability $R(\omega, L)$ for a plasmon to be scattered from one edge to the other. This can be achieved through high frequency noise measurement which are now available within the GHz domain and with a typical bandwidth down to 50 MHz [15].
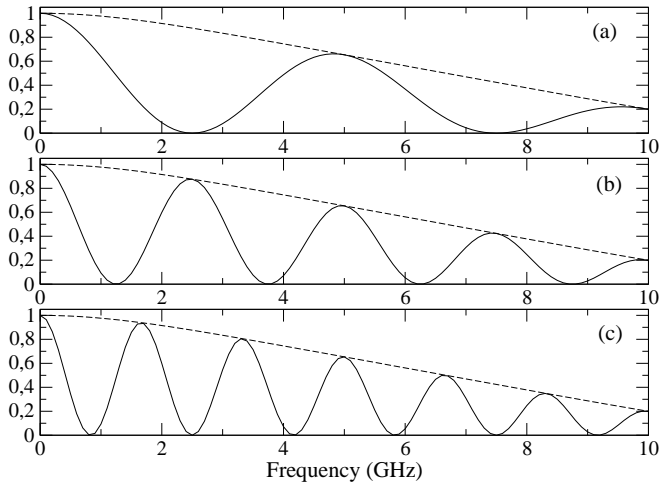
The finite frequency excess noise for the currents $I_{1'}$

FIG. 4: Prediction for the frequency dependence of $S_{i_1(L)}^{(\text{exc})}(\omega)/S_{i_1(L)}^{(\text{exc})}(\omega = 0)$ in the $0 - 10$ GHz range for $V = 50$ μV and (a) $L = 10$, (b) 20 and (c) 30 μm. The electronic temperature is fixed to $T_{\text{el}} = 30$ mK. We have assumed $v = 10^5$ ms^{-1} and $\theta = \pi/2$. Dashed lines show the non equilibrium excess noise produced by the QPC (no relaxation).

and $I_{2'}$ entering Ohmic contacts gives access to the edge current excess noises $(S_{i_{\alpha}(L)}^{(\text{exc})}(\omega))_{\alpha=1,2}$ since $S_{i_{\alpha}(L)}^{(\text{exc})}(\omega) = S_{I_{\alpha'}}(\omega, V) - S_{I_{\alpha'}}(\omega, V = 0)$ for $\alpha = 1, 2$. All ohmic contacts being at temperature T_{el}, after a distance L, the symmetric edge current excess noises read:

$$S_{i_1(L)}^{(\text{exc})}(\omega) = T(\omega, L)\, S_{i_1(0)}^{(\text{exc})}(\omega) \tag{11}$$

$$S_{i_2(L)}^{(\text{exc})}(\omega) = R(\omega, L)\, S_{i_1(0)}^{(\text{exc})}(\omega), \tag{12}$$

where $S_{i_1(0)}^{(\text{exc})}(\omega)$ is given by (9). Using the low energy scattering matrix (4), oscillations as a function of fre-

quency are expected. Accessing 4 to 8 GHz frequencies requires $|V| \geq 50$ μV and $L \geq 20$ μm to exhibit at least two oscillations. Fig. 4 depicts $S_{i_1(L)}^{(\text{exc})}(\omega)/S_{i_1(L)}^{(\text{exc})}(0)$ calculated for various L at fixed V, assuming $v \simeq 10^5$ ms^{-1} and $\theta = \pi/2$. The zero frequency excess noise $S_{i_1(L)}^{(\text{exc})}(0) = e^2 \mathcal{R}\mathcal{T} \frac{eV}{h} \left(\coth\left(eV/2k_B T_{\text{el}}\right) - 2k_B T_{\text{el}}/eV \right)$ is left unaffected by interactions since $\mathbf{S}(\omega = 0, L) = \mathbf{1}$.

In this Letter we have addressed the issue of accessing plasmon scattering in $\nu = 2$ edge states through energy exchange measurement and finite frequency noise. We have argued that a universal low energy plasmon scattering matrix can be derived for systems with screened Coulomb interactions. Comparing predictions obtained from this matrix with recent experimental data, we argue that this approach adequately captures most of the physics of energy exchange in this system and discuss possible explanations [18, 19, 20] to the small discrepancy between experimental data and our model. We then argue that high frequency noise provides a direct probe of plasmon scattering and that its measurement would lead to a deeper understanding of the validity and limits of the plasmon model. Finally, let us stress that sample design could be used to modulate inter channel interactions, thus leading to the realization of plasmon beam splitters, a building block for magnetoplasmon quantum optics.

Note: During completion of this work we became aware of related work by A. M. Lunde *et al.* [24] based on the iteration of a collision approach for short distance equilibration by Coulomb interactions.

[1] G. Fève *et al*, Science **316**, 1169 (2007).
[2] Y. Ji *et al*, Nature **422**, 415 (2003).
[3] S. Ol'khovskaya *et al*, Phys. Rev. Lett. **101**, 166802 (2008).
[4] I. Safi, Eur. Phys. J. D **12**, 451 (1999).
[5] R. Fazio, Phys. Rev. Lett. **80**, 5611 (1998).
[6] C. Kane and M. Fisher, Phys. Rev. Lett. **76**, 3192 (1996).
[7] I. Levkivskyi and E. Sukhorukov, Phys. Rev. B **78**, 045322 (2008).
[8] P. Degiovanni, C. Grenier, and G. Fève, http://arxiv.org/abs/0907.2996.
[9] I. Neder *et al*, Phys. Rev. Lett. **96**, 016804 (2006).
[10] P. Roulleau *et al*, Phys. Rev. B **76**, 161309 (2007).
[11] P. Roulleau *et al*, Phys. Rev. Lett. **101**, 186803 (2008).
[12] P. Roulleau *et al*, Phys. Rev. Lett. **100**, 126802 (2008).
[13] J. Gabelli *et al*, Science **313**, 5786 (2006).
[14] J. Gabelli *et al*, Phys. Rev. Lett. **98**, 166806 (2007).
[15] E. Zakka-Bajjani *et al*, Phys. Rev. Lett. **99**, 236803 (2007).

[16] C. Altimiras *et al*, Non equilibrium edge channel spectroscopy in the integer quantum Hall regime, Nature Physics, in press (2009).
[17] H. le Sueur *et al*, in preparation.
[18] C. de C. Chamon and X.G. Wen, Phys. Rev. B **49**, 8227 (1994).
[19] J. Han and D. Thouless, Phys. Rev. B **55**, R1926 (1997).
[20] I. Aleiner and L. Glazman, Phys. Rev. Lett. **72**, 2935 (1994).
[21] M. Büttiker, Phys. Rev. B **38**, 9375 (1988).
[22] T. Christen and M. Büttiker, Phys. Rev. B **53**, 2064 (1996).
[23] M. Büttiker, Phys. Rev. Lett. **57**, 1761 (1986).
[24] A. M. Lunde, S. E. Nigg, and M. Büttiker, preprint (2009).
[25] Plasmon scattering is elastic because of the quadratic form of Coulomb interactions in the bosonic field Φ.